Vacuum 193 (2021) 110504

Contents lists available at ScienceDirect

Vacuum

journal homepage: www.elsevier.com/locate/vacuum

Surface erosion by moving ion beam

A.S. Rudy [a,*], A.N. Kulikov [b], V.I. Bachurin [a]

[a] Valiev Institute of Physics and Technology of Russian Academy of Sciences, Yaroslavl Branch, St., 21, 150007, Russian Federation
[b] Yaroslavl State University, Sovetskaya St., 14, 150000, Russian Federation

ARTICLE INFO

Keywords:
Sputtering
Moving ion beam
Boundary value problem
State of equilibrium
Discontinuous solution

ABSTRACT

A mathematical model of surface erosion in a course of a trench formation by translationally moving ion beam of a Gaussian shape is considered. The solutions obtained in self-similar variables describe the states of equilibrium of the boundary value problem and their dependence on the sputtering parameters. It is shown that there are three parameter areas in which only smooth, smooth and discontinuous and only discontinuous solutions exist. The plots of the surface profiles corresponding to three possible types of solutions are given. Formulas for calculating the profile of etching trenches and examples of calculating profiles corresponding to smooth and discontinuous solutions are given.

1. Introduction

In the course of solid's surface bombardment by high energy ions the removal of the external atomic layers of the target occurs. This phenomenon, known as surface erosion, is widely used as a standard technique in the secondary ion mass spectrometry for depth profiling, and in micro- and nanotechnologies. As the rate of an infinitesimal surface area sputtering depends on the local angle of bombardment, erosion may considerably modify initial surface microtopography.

A review of the first works on the relief formation on the surface of solids under the ion bombardment can be found in the book by R. Behrish [1]. Theoretical approaches to this phenomenon based on the angular dependence of the sputtering yield were formulated in the review by G. Carter [2]. More recent interest in the study of surface relief formation was due to the possibility of creating ripples and ordered wave-like structures of micron and nanometer scale on the surface of a number of materials. A fairly detailed review of the experimental results and mechanisms of ripple formation is presented in Ref. [3].

To date, several models have been developed for surface structuring during its ion sputtering. In the work by Carter and Vishnyakov [4], the possibility of directed redistribution of the mass by recoil atoms in a collision cascades and of the angular dependence of the sputtering yield were considered. Bradley and Harper evolving Sigmund's theory of sputtering [5] proposed a linear model of ripple formation [6] based on the angular dependence of erosion and on the concept of surface diffusion. Simulation of the parameters of periodic structures by the Monte Carlo method, based on the models [4,6] under various conditions of ion bombardment, reveals good agreement with the experimental results [7,8]. Nonlinear models for the formation of periodic structures were proposed in Refs. [9–11]. In works [12,13] the hydrodynamic approach to ripples formation in the surface layer amorphized by ion bombardment was developed. The paper [14] presents a nonlocal erosion model based on P. Sigmund theory, but taking into considering the spatial nonlocality of the sputtering implying that the points of the primary ion impact and the secondary ion emission are spatially shifted. It should be noted that practically in all these works, both experimental and theoretical, the ion fluence at the sample surface was assumed to be homogeneous.

In the early 2000s, was developed a method for the formation of a regular wavy nanorelief [15] by a moving ion beam. To form an array of ordered waves a ribbon ion beam moving translationally at a constant rate was used. When moving the beam forms a trench with a slope in its front part (Fig. 1) where the local angle of bombardment $\Theta - \Theta_0$ may fall in the region of a wavy nanorelief existence. In this event an array of a coherent nanometer waves is formed at the bottom of the trench. The essence of the method is that due to the dependence of the wavelength on the angle of bombardment Θ_0, the condition of the relief formation is fulfilled only for waves of a certain length, which ensure their high coherence. It was supposed that by changing the speed of the ion beam, the fluence, or the angle of bombardment, it would be possible to obtain slopes of various steepness, thereby adjusting the wavelength. The analysis of the erosion equation, considered in its most general form [2,16], shows that this is far from the case.

It seems obvious that a slowly moving beam of a given intensity and

* Corresponding author.
E-mail address: rudy@uniyar.ac.ru (A.S. Rudy).

https://doi.org/10.1016/j.vacuum.2021.110504
Received 10 March 2021; Received in revised form 28 July 2021; Accepted 30 July 2021
Available online 2 August 2021

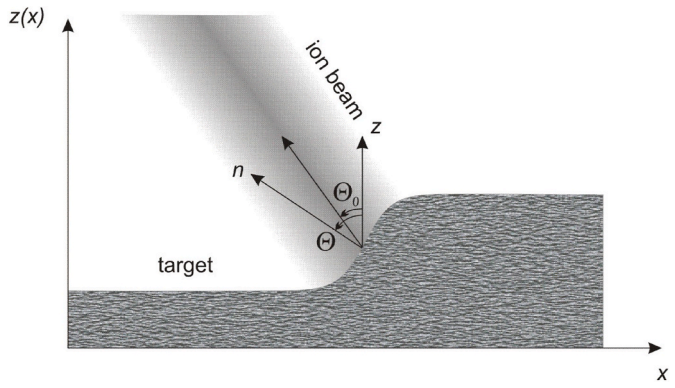

Fig. 1. Side-view of flat surface sputtered by a moving ribbon ion beam.

angle of incidence should form a trench of a strictly definite depth. However, and this will be shown below, in a certain range of ion beam parameters there is no unambiguous relationship between sputtering parameters and the trench depth. At a certain value of the beam velocity, fluence or bombardment angle, the monotonous trench depth dependence on these parameters undergoes a break, so some depth values, as well as local angles of bombardment will simply be unattainable. The reasons for such peculiarities of a surface sputtering by moving ion beam become clear when analysing the mathematical model below.

1. Equation of surface erosion by moving ion beam and its solution

To describe the process of surface erosion by an ion beam, many models have been proposed, the main of which were mentioned above. As a rule, all of them are the results of consideration more subtle effects of sputtering within the framework of the basic model

$$\frac{\partial z}{\partial t} = -\frac{1}{\rho} J V(\Theta) \tag{1}$$

presented in Refs. [2,16] and a number of other works. Here derivative in the left-hand side of equation stands for the local rate of surface height $z(x,t)$ reduction. This rate is determined by the fluence $\boldsymbol{J}$ of incident ions, averaged both over the time and the space variables, atomic density of target ρ and some function

$$V(\Theta) = Y(\Theta_0 - \Theta)\frac{\cos(\Theta_0 - \Theta)}{\cos\Theta} \tag{2}$$

where $Y(\Theta_0 - \Theta)$ is sputtering yield, Θ_0 is the angle between $\boldsymbol{z}$-axis and bombardment direction, Θ is the angle between $\boldsymbol{z}$-axis and local normal to a surface element. In the case of surface sputtering by stationary ion beam its fluence is a single valued and limited function of coordinate which meets the boundary condition

$$J(x) \to 0, \quad x \to \pm\infty \tag{3}$$

At surface sputtering by moving beam fluence $\boldsymbol{J}$ is a time-dependent function $J(x - vt)$, where $\boldsymbol{v}$ is a beam velocity. Consider the case when the density of the ion beam is described by the Gaussian function, which in a fixed coordinate system has the form

$$J(x - vt) = J_0 \exp\left[-\frac{(x - vt)^2}{\delta^2}\right] \tag{4}$$

By differentiating Eq. (1) on $\boldsymbol{x}$ and changing in left-hand side the order of differentiation it easy to get the following nonlinear hyperbolic equation

$$\frac{\partial}{\partial t}(\tan\Theta) = -\cos^2\Theta\frac{\partial}{\partial x}\left[\frac{J(x - vt)}{\rho}V(\Theta)\right] \tag{5}$$

which must be considered together with the supplemental condition

$$\frac{\partial z}{\partial x} = \tan\Theta \tag{6}$$

Further, two variants of studying the system of equations (5) and (6) are possible: the statement of the Cauchy problem and its analysis, or the statement and analysis of the boundary value problem. If system (5), (6) is supplemented with initial conditions $\Theta(x,t_0) = \Theta_0(x)$, $z(x,t_0) = z_0(x)$ then it can be solved by a standard method referred to as the method of characteristics, a description of which can be found in Refs. [2,16,17]. As shown by E. Hopf [18], solutions of this problem can be discontinuous functions (ambiguous solutions), which in physics are referred to as shock waves. In present case, we offer an alternative approach in which our solution is recast as a traveling wave problem for which the boundary conditions

$$\Theta \to 0, \quad \xi \to \pm\infty \tag{7}$$

are essential. Therefore, it is precisely the boundary value problem (5) - (7) that is considered below, for which solutions in the form of traveling waves are sought.

It is natural to seek a solution to the boundary value problem (5) - (7) in the class of self-similar solutions, for which it is necessary to perform Galilean transformation $\xi = (x - vt)/\delta$, reducing Eq. (5) to

$$\frac{\partial}{\partial\xi}\left[\frac{1}{v\rho}J(\xi)V(\Theta) - \tan\Theta\right] = 0 \tag{8}$$

where $J(\xi) = J_0\exp(-\xi^2)$. Obviously, the expression in parentheses is a constant

$$\frac{J_0}{v\rho}\exp(-\xi^2)V(\Theta) - \tan\Theta = C \tag{9}$$

and by virtue of condition (7) $C = 0$. After obvious reductions, taking into consideration Eq. (2), Eq. (9) acquires the form

$$\xi = \pm\sqrt{\ln\left[\frac{J_0}{v\rho}\frac{Y(\Theta_0 - \Theta)\cos(\Theta_0 - \Theta)}{\sin\Theta}\right]} \tag{10}$$

The latter can be resolved numerically as $\xi(\Theta)$ and inverted to obtain sought-for solution $\Theta(\xi)$, providing the sputtering yield $Y(\Theta)$ is a known function.

Sputtering yield angular dependence $Y(\Theta)$, strongly varying for a different target materials and ion beam parameters, in all further examples is calculated for the case of silicon sputtered by 9 keV nitrogen N_2^+ ions. Experimentally obtained dependence $Y(\Theta)$ [19] was approximated by Yamamura function [20].

$$Y(\Theta) = Y(0)\frac{\exp(\alpha - \alpha/\cos\Theta)}{\cos^{\beta}\Theta} \tag{11}$$

where α and β are parameters of Eq. (11) that provide the best fit for experimental points

$$\alpha = \frac{\ln[Y_{\max}/Y(0)]\cos\Theta_{\max}}{\cos\Theta_{\max} - \ln(\cos\Theta_{\max}) - 1}\cdot\beta = \frac{\alpha}{\cos\Theta_{\max}} \tag{12}$$

and where $\Theta_{\max}$ matches up sputtering yield maximum.

Considering Eqs. (11) and (12), Eq. (10) can be reduced to

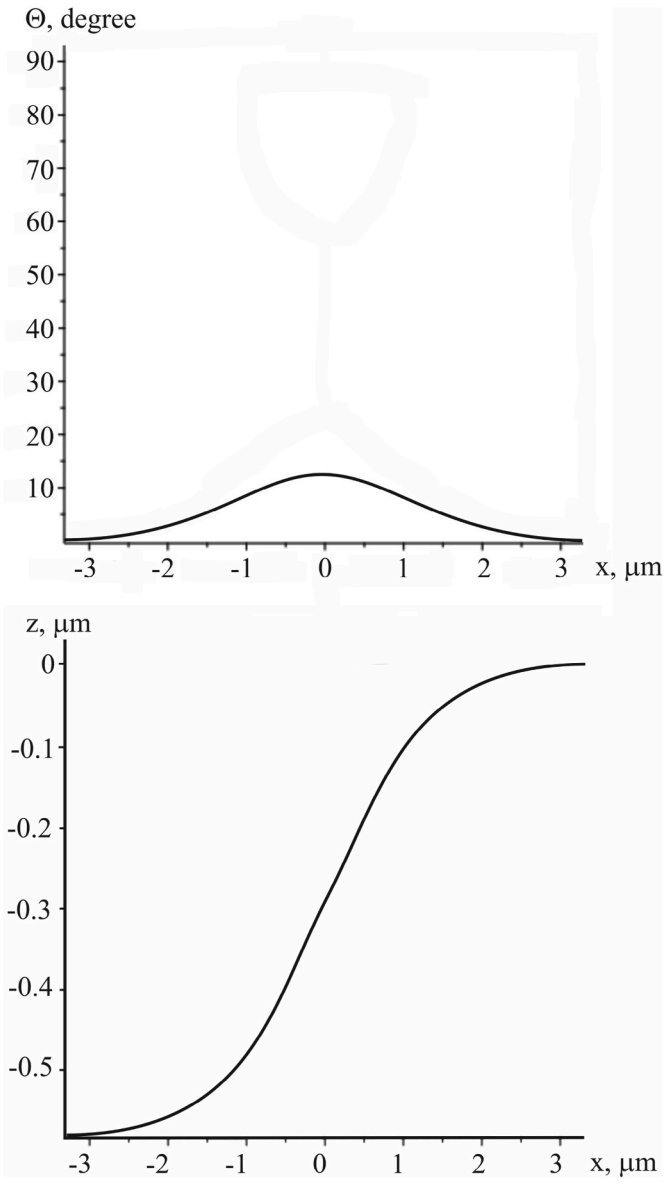

Fig. 2. Plots $\Theta(x)$ and $z(x)$ at the first critical value of the control parameter $A_1 = 0.67666$. In the parameter range $0 < A < A_1$, the function $\Theta(x)$ is unambiguous, and $z(x)$ is smooth.

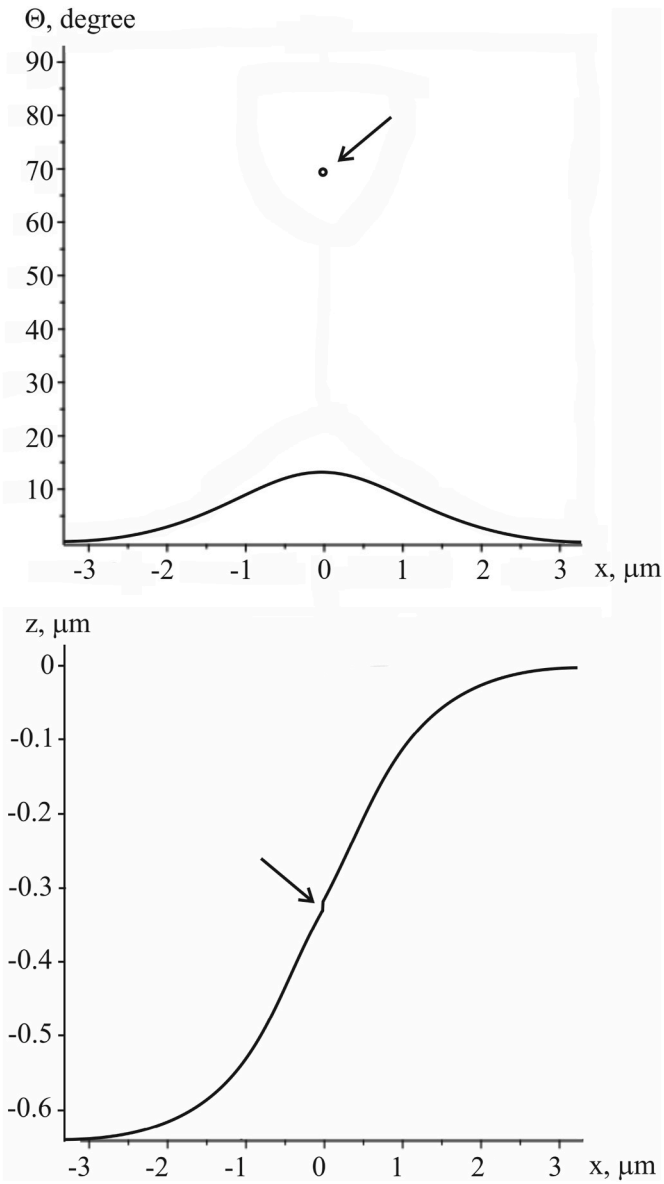

Fig. 3. Plots $\Theta(x)$ and $z(x)$ in the supercritical region $A = 0.67690 > A_1$. The arrows show the region where the function $\Theta(x)$ is ambiguous and the corresponding discontinuity on the curve $z(x)$.

$$\xi = \pm\sqrt{\ln\left(A\frac{\exp[-\alpha/\cos(\Theta_0-\Theta)]}{\sin\Theta\cos^{\beta-1}(\Theta_0-\Theta)}\right)} \tag{13}$$

where the sputtering parameters are combined into a dimensionless complex $A = J_0 Y(0)\exp\alpha/\nu\rho$. Such complexes, analogous to similarity numbers and determining the behavior of a dynamical system, are usually called control or bifurcation parameters. The latter term is used in cases when bifurcation of new solutions takes place when the control parameter exceeds a certain critical value.

The numerical solution of Eqs. (13) and (6) in a certain range of the parameter $\boldsymbol{A}$ values leads to an ambiguous dependence $\Theta(\xi)$, which means that the corresponding solution $z(\xi)$ is a piecewise continuous function. Thus, the problem arises of determining the range of parameter $\boldsymbol{A}$ values in which discontinuous solutions take place [21] and the choice of stable solutions. A rigorous analytical solution to this problem is given in the Appendix. Below are the results of the numerical solution of Eq. (13), which are interpreted in light of a more rigorous analysis of Eq. (5) provided in Appendix.

2. Examples of discontinuous surfaces

By tabulating Eq. (13), one can obtain an array $\xi_i(\Theta_i)$ for any desired value of the control parameter $\boldsymbol{A}$ and convert it to $\Theta_i(x_i)$. Using the sequence $\Theta_i(x_i)$ and Eq. (6) it is easy to reconstruct the surface profile

$$z(x) = \int_{-\infty}^{x} \tan\Theta(x)dx \tag{14}$$

by numerical integration. The resulting dependencies $\Theta(x)$ and $z(x)$ may be both unambiguous and smooth or ambiguous and discontinuous,

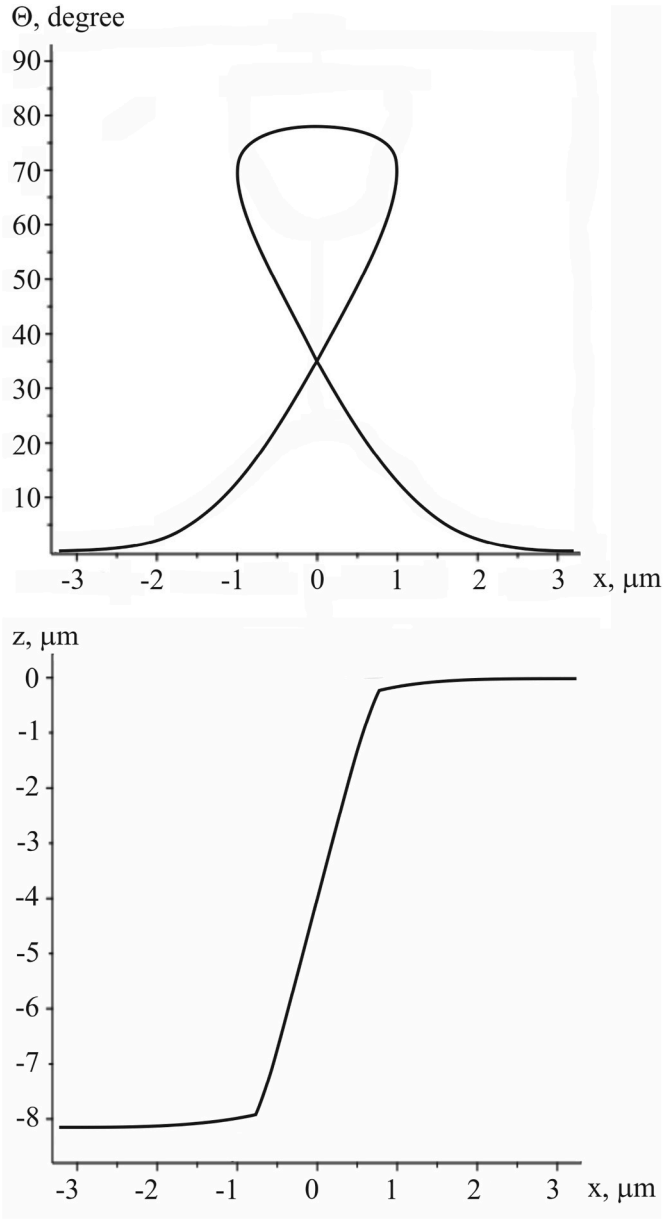

Fig. 4. Plots $\Theta(x)$ and $z(x)$ at the second critical value of the control parameter $A_2 = 1.17315$.

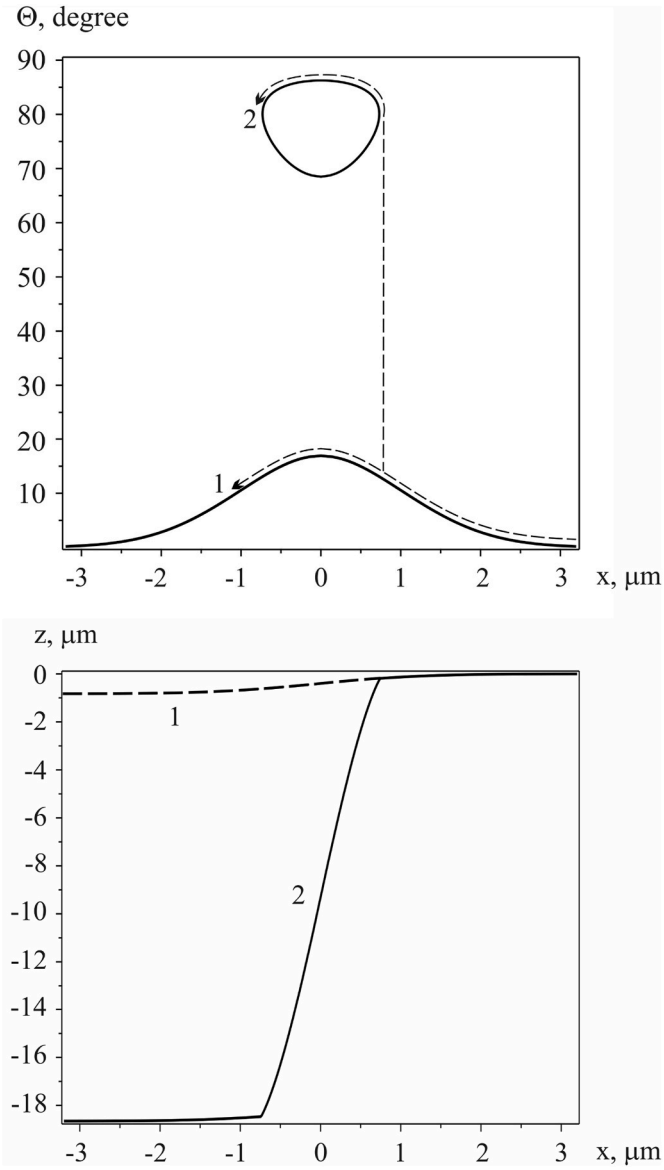

Fig. 5. Plots $\Theta(x)$ and discontinuous solution $z(x)$ at $\Theta_0 = 10^\circ$ and $A = 0.9$. Arrows show the paths of Eq. (15) integration corresponding smooth 1 and discontinuous 2 solutions $z(x)$.

so for their interpretation, the results of the analysis given in the Appendix will be required. Figs. 2–4 show the profiles $\Theta(x)$ and $z(x)$ plotted in a moving frame for the control parameter values $A = A_1 = 0.67666$, $A = 0.67690$, $A = A_2 = 1.17315$, and the angle of bombardment $\Theta_0 = 0^\circ$. Fig. 5 provides an example of trench profile for nonzero angle of beam incidence $\Theta_0 = 10^\circ$ at $A = 0.9$.

Fig. 2 shows the plots of Eqs. (13) and (14) corresponding to the solution of an auxiliary equation $u_s(\eta), \quad u \in F_0P_0, \quad \eta \in (0,1)$ at $A = A_1$ considered in Appendix (Eq. (A14)). In this case, the functions $\Theta(x)$ and $z(x)$ are smooth and unambiguous. However, when the critical parameter is slightly exceeded $\varepsilon = (A - A_1)/A_1 = 0.00035$, on the plot of the function $\Theta(x)$ in the vicinity of the point $M(0, 69.4^\circ)$ a small domain of Eq. (13) solution appears and the solution $z(x)$ becomes a piecewise continuous function (Fig. 3). Fig. 4 shows the plots of functions $\Theta(x)$ and $z(x)$ for $A = A_2$, when smooth solutions $u_s(\eta)$ of an auxiliary equation disappear and only piecewise continuous solutions $u_d(\eta)$, considered in the Appendix, remain. It is essential that the trench in the case of discontinuous solutions is an order of magnitude deeper than in the case of smooth solutions.

If the angle of bombardment is nonzero, the critical values of parameter $\boldsymbol{A}$ also undergo a corresponding alteration. Fig. 5 shows the plots $\Theta(x)$ and $z(x)$ for the bombardment angle $\Theta_0 = 10^\circ$. It is obvious that in this case $A \in [A_1', A_2']$, where A_1' and A_2' are some new critical values of the control parameter. However, the general scheme of system evolution at control parameter variation, considered in the Appendix, remains the same as for $\Theta_0 = 0^\circ$.

3. Summary

In the course of analysis of the problem on surface sputtering by

moving ion beam, both smooth and discontinuous solutions of "traveling wave" and "shock wave" types, have been obtained. This result reflects a fundamental property of the systems modeled by equations (5)–(7), referred to as bistability. This property does not depend on the method for solving the problem, and in the case of the Cauchy problem solved by the characteristics method, along with smooth solutions, solutions that are ambiguous in terms of $\Theta(x,t)$ and discontinuous in terms $z(x,t)$ most likely will be obtained. A similar situation arises when analyzing the well-known Hopf equation

$$\frac{\partial u}{\partial t}+u\frac{\partial u}{\partial x}=0 \tag{15}$$

which is characterized by discontinuous solutions [18]. Equation (5) belongs to the same class as the Hopf equation, with the difference that equation (5) is much more complicated.

The most important for practical application result is the revealed relationship of wave's amplitude and control parameter value. According this result trench's profile and depth may be controlled by $\boldsymbol{A}$ parameter adjustment, but only within a certain limit. With parameter $\boldsymbol{A}$ variation and compliance with the condition $A < A_1$ the trench depth

$$h=\int_{-\infty}^{\infty} tg\Theta(x)dx \tag{16}$$

varies monotonically. Within domain $[A_1, A_2]$ there are two feasible solutions $z(x)$: smooth 1 and discontinuous 2 (Fig. 5). The results of the analysis given in the Appendix do not answer the question which of the two solutions will be stable, i.e. which of the two sputtering regimes will occur in the technological process. If one of the solutions is unstable, then during the trench formation, a spontaneous change in the sputtering regime can occur despite the fixed parameters of the ion beam. For example, the transition from a high sputtering rate at large angles Θ (Fig. 5, curve 2) when a deep trench is formed, to a low sputtering speed with a small angle profile $z(x)$ and shallow trench is possible. And finally, at $A > A_2$, only one discontinuous solution remains, to which in practice correspond deep trenches.

This study was performed in accordance with a State assignment of the Ministry of Education and Science of the Russian Federation to Valiev Institute of Physics and Technology, Yaroslavl Branch, Russian Academy of Sciences # 75-00669-21-00 of 23.12.2020.

Declaration of competing interest

The authors declare that they have no known competing financial interests or personal relationships that could have appeared to influence the work reported in this paper.

Appendix

A1. Analysis of erosion equation solutions

Let us rewrite Eq. (5) in self-similar variables and introduce new notation $\tan\Theta = u$. Further consideration will be carried out for normal bombardment, when $\Theta_0 = 0$ and assumption that condition $\Theta \in (-\pi/2, \pi/2)$ always holds. In this case relation $\Theta = \arctan(u)$ is always valid and Eq. (15) subject to relation $\cos\Theta = 1/\sqrt{1+u^2}$ and boundary condition (9) may be written in a new designation as

$$A\exp\left(-\xi^2\right)\exp\left(-\alpha\sqrt{1+u^2}\right)\left(1+u^2\right)^{\frac{\beta}{2}}-u=0 \tag{A1}$$

Function $u(\tau,\xi)$ in Eq. (A1) may be considered as a product of two functions

$$u=A\eta(\xi)G(u) \tag{A2}$$

where

$$\eta\left(\xi\right)=\exp\left(-\xi^2\right)\in(0;1] \tag{A3}$$

and

$$G(u)=\exp\left(-\alpha\sqrt{1+u^2}\right)\left(1+u^2\right)^{\frac{\beta}{2}} \tag{A4}$$

Function $G(u)$ is a bounded one as according equation

$$G_u^{'}(u)\equiv G(u)\frac{u}{\sqrt{1+u^2}}\left(\frac{\beta}{\sqrt{1+u^2}}-\alpha\right) \tag{A5}$$

it has maximum at $\sqrt{1+u^2}=\beta/\alpha$. From here follows inequality

$$0<G(u)\le M=\exp(-\beta)\left(\frac{\beta}{\alpha}\right)^{\beta} \tag{A6}$$

which by virtue of Eq. (A2) yields condition

$$0<u(\eta)<AM\eta \tag{A7}$$

implying that with all admissible η, thus with all ξ, function (A4) is a bounded one.

To apply implicit function theorem let us reduce Eq. (A2) to

$$\eta = \frac{1}{A}\frac{u}{G(u)} \tag{A8}$$

and find its derivative over $\boldsymbol{u}$

$$\frac{\partial \eta}{\partial u} = \frac{1}{A}\frac{G(u) - uG_u'(u)}{G^2(u)} \tag{A9}$$

Subject to Eq. (A4), which can be rewritten as $G_u'(u) = G(u)\phi(u)$, Eq. (A9) reduces to

$$\frac{\partial \eta}{\partial u} = \frac{1}{A}\frac{1 - u\phi(u)}{G(u)} \tag{A10}$$

where

$$\phi(u) = u\frac{\beta - \alpha\sqrt{1+u^2}}{1+u^2} \tag{A11}$$

According implicit function theorem, in the points where Eq. (A10) r.h.s. is nonzero, in sufficiently small vicinity of any solution (η_0, u_0) of Eq. (A8) there exists sufficiently smooth solution $u = u(\eta)$ of this equation. For instance, in a vicinity of formal solution $(0, 0)$ exists the single state of equilibrium of boundary value problem (8), (9) (i.e. single running wave). In the point where $\partial\eta/\partial u = 0$ implicit function theorem is inapplicable, what admits an ambiguous solution of Eq. (A8).

To reveal these points let us set Eq. (A10) equal to zero

$$1 - u\phi(u) = 0 \tag{A12}$$

thereby it reduces to equation free from parameter $\boldsymbol{A}$, which roots does not already depend on control parameter. Substitution of Eq. (A11) and new designation $1 + y = \sqrt{1+u^2}$, signifying that $y \geq 0$, in Eq. (A12) yields cubic equation

$$\alpha y^3 + (1 - \beta + 3\alpha)y^2 + 2(1 + \alpha - \beta)y + 1 = 0 \tag{A13}$$

Analysis reveals that Eq. (A13) has two positive roots y_1, y_2 relating to Eq. (A12) roots as $u_1 = 2.691545$ and $u_2 = 0.701918$.

Points u_1 and u_2 correspond to function's $u/G(u)$ maximum $u_2/G(u_2) = 1.17315$ and minimum $u_1/G(u_1) = 0.67666$ respectively. Whereas $\eta \leq 1$, $\boldsymbol{A}$ values $A_1 = 0.67666$ and $A_2 = 1.17315$, matching up conditions $\eta(u_1) = 1$ and $\eta(u_2) = 1$ (see Eq. (A8)), may be considered as control parameter critical values, determining the main three situations.

I. With $A < A_1$ Eq. (A8) has single solution, shown in Fig. A1

II. Within the interval $A_1 < A < A_2$ Eq. (A8) solution is already ambiguous. For each $\eta_0 \in (0, \eta_1)$ equation (Fig. A2) has single solution, at $\eta_0 \in (\eta_1, 1)$ it has three solutions, and at $\eta_0 = \eta_1$ it has two solutions. I.e. Eq. (A8) has continuum solutions, including those that have finite number of discontinuity points.

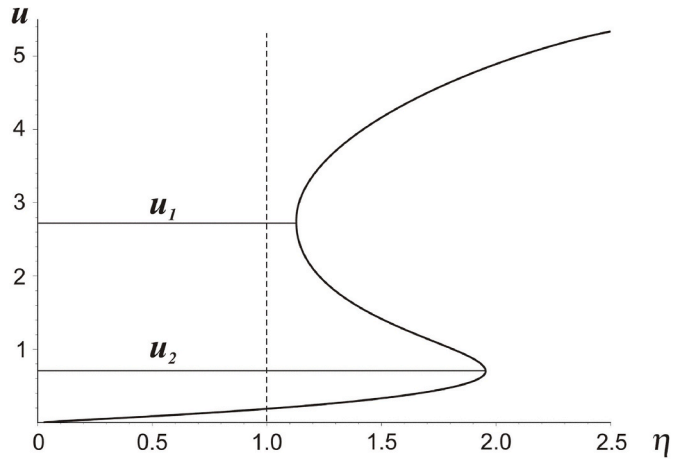

Fig. A1. Plot of function $u(\eta)$ in precritical domain $A < A_1$. Eq. (A8) has single solution corresponding to lower branch of the curve.

Here are five examples of possible solutions:
four discontinuous solutions

$$1)\quad u=u(\eta)=\begin{cases} u,u\in F_0F_1,\eta\in(0,\eta_1) \\ u,u\in F_3F_4,\eta\in[\eta_1,1] \end{cases} \tag{A14}$$

$$2)\quad u=u(\eta)=\begin{cases} u,u\in F_0F_1,\eta\in(0,\eta_1) \\ u,u\in F_3P_4,\eta\in[\eta_1,1] \end{cases} \tag{A15}$$

$$3)\quad u=u(\eta)=\begin{cases} u,u\in F_0P_1,\eta\in(0,\eta_*) \\ u,u\in P_3F_4,\eta\in(\eta_*,1] \end{cases} \tag{A16}$$

$$4)\quad u=u(\eta)=\begin{cases} u,u\in F_0P_1,\eta\in(0,\eta_*) \\ u,u\in P_2P_4,\eta\in(\eta_*,1] \end{cases} \tag{A17}$$

and one smooth solution

$$5)\quad u=u(\eta),\quad u\in F_0P_0,\quad \eta\in(0,1) \tag{A18}$$

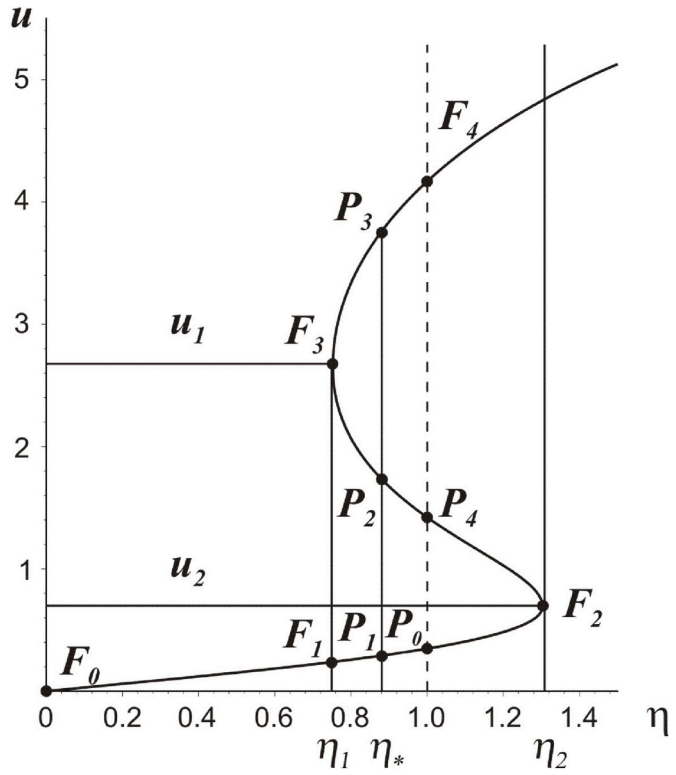

Fig. A2. Plot of function $u(\eta)$ within critical values $A_1 < A < A_2$. Eq. (A8) has continuum of discontinuous and one smooth solution.

In Eqs. (A14) – (A18) the expression in the r.h.s. ($u(\eta) = u,\ \ u \in F_0, F_1$ for instance) signifies that solution belongs to F_0, F_1 brunch in Fig. A2. As further both variants 1) and 5) will play the particular role, let us denote solutions 1) as $u_d(\eta)$ and solution 5) as $u_s(\eta)$.

III. When $A > A_2$ (Fig. A3), as well as in previous case, solution of Eq. (A8) is ambiguous but in contrast with **II** the smooth solution disappears. From the infinite set of solutions for further consideration will be chosen only one

$$u=u(\eta)=\begin{cases} u,u\in F_0F_1,\eta\in(0,\eta_1) \\ u,u\in F_3F_4,\eta\in[\eta_1,1] \end{cases} \tag{A19}$$

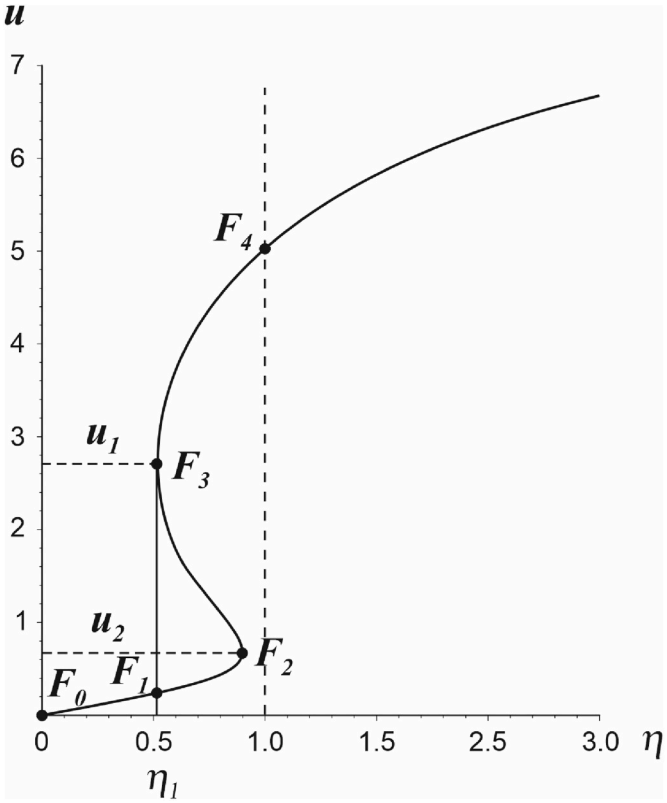

Fig. A3. Plot of function $u(\eta)$ in supercritical domain $A > A_2$. Eq. (A8) has continuum of discontinuous solutions.

It is noteworthy that all solutions of Eq. (A8) belong to the class of generalized solutions of Eq. (8) [21–23], i.e. to the class of functions meeting the following conditions:

- In any bounded half-plane $\tau \geq 0$ a number of lines and points of discontinuity of a function $u(\tau, \xi)$ is finite. Outside these lines and points function $u(\tau, \xi)$ is continuously differentiable over each variable.
- At lines of discontinuity one-sided derivatives of $u(\tau, \xi)$ exist.

Existence of above defined solutions was proved in the works by O.A. Oleinik [21–23].

A2. Stability of solutions obtained

As is well known, physically feasible are only generalized solutions that are resistant to small perturbations. As applied to the problem in question this means that stable discontinuous solutions should satisfies inequality

$$f_u'[\xi_+, u(\xi_+)] \leq 0 \leq f_u'[\xi_-, u(\xi_-)] \tag{A20}$$

where $\xi_+ = \xi_* + 0$, $\xi_- = \xi_* - 0$, and ξ_* is discontinuity point. This stability criterion is applicable only provided that

$$f_{uu}'' \neq 0 \tag{A21}$$

It is easy to verify that in present instance this condition always holds. According dependence $f_{uu}''(u)/A\eta$ second derivative makes vanish in points $u_3 = 1.8978$ and $u_4 = 5.6248$, i.e. far from extremum points u_1, u_2.

It is also significant that derivate

$$f_u' = A\eta G(u)\phi(u) - 1 \tag{A22}$$

vanishes when $u\phi(u) = u/A\eta G(u) \equiv 1$, hence

$$\boldsymbol{sign}\, f_u' = -\boldsymbol{sign}\left(\frac{\boldsymbol{u}}{\boldsymbol{G(u)}}\right)_{\boldsymbol{u}}' \tag{A23}$$

This implies that among solutions of Eq. (A8) should be chosen those $u(\eta)$ for which function $u/G(u)$ in discontinuity point has minimal value. Here the corresponding solution is monotone increasing function of η, which derivative in discontinuity point η_* meets Eq. (A20)

$$\lim_{\eta \to \eta - 0} u'(\eta) > 0 \tag{A24}$$

while

$$\lim_{\eta \to \eta + 0} u'(\eta) = +\infty \tag{A25}$$

Thus, among continuum of states of equilibrium, given by piecewise continuous functions in the case **II** only solutions $u_d(\eta)$, as well as $u_s(\eta)$ are feasible. The same situation takes place in the case **III** with the only difference that there is no smooth solution. In the case **I**, vice versa, only smooth solution $u_s(\eta)$ is feasible.

References

[1] Behrisch (Ed.), Sputtering by Particle Bombardment II, Springer, 1983.
[2] G. Carter, The physics and applications of ion beam erosion, J. Phys. D Appl. Phys. 34 (2001) (Rl).
[3] J. Munoz-Garcia, L. Vazquez, M. Castro, R. Cago, A. Redondo-Cubero, A. Moreno-Barrado, R. Cuerno, Self-organized nanopatterning of silicon surfaces by ion beam sputtering, Mater. Sci. Eng., R 86 (2014) 1.
[4] G. Carter, V. Vishnyakov, Roughening and ripple instabilities on ion-bombarded Si, Phys. Rev. **B** 54 (1996) 17647.
[5] P. Sigmund, A mechanism of surface micro-roughening by ion bombardment, J. Mater. Sci. 8 (1973) 1545.
[6] R.M. Bradley, J.M.E. Harper, Theory of ripple topography induced by ion bombardment, J. Vac. Sci. Technol. A 6 (1988) 2390.
[7] H. Hofsass, Surface instability and pattern formation by ion-induced erosion and mass redistribution, Appl. Phys. A 114 (2014) 401–422.
[8] H. Hofsass, O. Bobes, Prediction of ion-induced nanopattern formation using Monte Carlo simulations and comparison to experimentsб Appl, Phys. Rev. 6 (2019), 021307.
[9] M. Kardar, G. Parisi, Y.-C. Zhang, Dynamic scaling of growing interfaces, Phys. Rev. Lett. 56 (1986) 889.
[10] S. Park, B. Kahng, H. Jeong, A.-L. Barabasi, Dynamics of ripple formation in sputter erosion: nonlinear phenomena, Phys. Rev. Lett. 83 (1999) 3486.
[11] M.A. Makeev, A.-L. Barabasi, Ion-induced effective surface diffusion in ion sputtering, Appl. Phys. Lett. 71 (1997) 2800.
[12] M. Castro, R. Cuerno, Hydrodynamic approach to surface pattern formation by ion beams, Appl. Surf. Sci. 258 (2012) 4171.
[13] J. Munoz-Garcıa, R. Cuerno, M. Castro, Coupling of morphology to surface transport in ion-beam irradiated surfaces: oblique incidence, Phys. Rev. B 78 (2008), 205408.
[14] A.S. Rudy, V.I. Bachurin, V.K. Smirnov, Nanoscale model of surface erosion by ion bombardment, Radiat. Eff. Defect Solid 161 (2006) 319.
[15] I.V. Zhuravlev, D.S. Kibalov, G.F. Smirnova, V.K. Smirnov, Wavy surface nanostructures formed in amorphous silicon films by sputtering with nitrogen ions, Tech. Phys. Lett. 29 (2003) 949.
[16] R. Smith, S.J. Wilde, G. Carter, I.V. Katardjiev, M.J. Nobes, The simulation of two dimensional surface erosion and deposition processes, J. Vac. Sci. Technol. B 5 (1987) 579.
[17] G.B. Witham, Linear and Nonlinear Waves, John Wiley & Sons, London, 1974, p. 636.
[18] E. Hopf, The partial differential equation $u_t + uu_x = \mu u_{xx}$, Commun. Pure Appl. Math. 3 (1950) 201.
[19] V.I. Bachurin, P.A. Lepshin, V.K. Smirnov, Angular dependences of surface composition, sputtering and ripple formation on silicon under N^{2+} ion bombardment, Vacuum 56 (2000) 241.
[20] Y. Yamamura, Shigeru Shindo, An empirical formula for angular dependence of sputtering yields, Radiat. Eff. 80 (1984) 57.
[21] O.A. Oleinik, Discontinuous solutions of non-linear differential equations, Uspekhi Mat. Nauk 12 (1957) 3.
[22] O.A. Oleinik, On the Cauchy problem for nonlinear equations in a class of discontinuous functions, Dokl. Akad. Nauk SSSR 95 (1954) 451.
[23] O.A. Oleinik, Uniqueness and stability of a generalized solution of the Cauchy problem for a quasilinear equation, Uspekhi Mat. Nauk 14 (1959) 165.